Title

Diacylglycerol-induced Membrane Targeting and Activation of Protein Kinase Cε MECHANISTIC DIFFERENCES BETWEEN PROTEIN KINASES Cδ AND Cε*

Journal

Journal of Biological Chemistry, 280(20)

ISSN

0021-9258

Authors

Stahelin, Robert V
Digman, Michelle A
Medkova, Martina
et al.

Publication Date

2005-05-01

DOI

10.1074/jbc.m411285200

THE JOURNAL OF BIOLOGICAL CHEMISTRY
Vol. 280, No. 20, Issue of May 20, pp. 19784–19793, 2005
Printed in U.S.A.

Diacylglycerol-induced Membrane Targeting and Activation of Protein Kinase Cε

MECHANISTIC DIFFERENCES BETWEEN PROTEIN KINASES Cδ AND Cε*

Received for publication, October 4, 2004, and in revised form, March 14, 2005
Published, JBC Papers in Press, March 15, 2005, DOI 10.1074/jbc.M411285200

Robert V. Stahelin, Michelle A. Digman‡, Martina Medkova§, Bharath Ananthanarayanan¶, Heather R. Melowic, John D. Rafter, and Wonhwa Cho‖

From the Department of Chemistry, University of Illinois, Chicago, Illinois 60607

Two novel protein kinases C (PKC), PKCδ and PKCε, have been reported to have opposing functions in some mammalian cells. To understand the basis of their distinct cellular functions and regulation, we investigated the mechanism of *in vitro* and cellular *sn*-1,2-diacylglycerol (DAG)-mediated membrane binding of PKCε and compared it with that of PKCδ. The regulatory domains of novel PKC contain a C2 domain and a tandem repeat of C1 domains (C1A and C1B), which have been identified as the interaction site for DAG and phorbol ester. Isothermal titration calorimetry and surface plasmon resonance measurements showed that isolated C1A and C1B domains of PKCε have comparably high affinities for DAG and phorbol ester. Furthermore, *in vitro* activity and membrane binding analyses of PKCε mutants showed that both the C1A and C1B domains play a role in the DAG-induced membrane binding and activation of PKCε. The C1 domains of PKCε are not conformationally restricted and readily accessible for DAG binding unlike those of PKCδ. Consequently, phosphatidylserine-dependent unleashing of C1 domains seen with PKCδ was not necessary for PKCε. Cell studies with fluorescent protein-tagged PKCs showed that, due to the lack of lipid headgroup selectivity, PKCε translocated to both the plasma membrane and the nuclear membrane, whereas PKCδ migrates specifically to the plasma membrane under the conditions in which DAG is evenly distributed among intracellular membranes of HEK293 cells. Also, PKCε translocated much faster than PKCδ due to conformational flexibility of its C1 domains. Collectively, these results provide new insight into the differential activation mechanisms of PKCδ and PKCε based on different structural and functional properties of their C1 domains.

Protein kinases C (PKC)[1] comprise a family of serine/threonine kinases that mediate a wide variety of cellular processes (1–3). All PKCs contain an amino-terminal regulatory domain and a carboxyl-terminal catalytic domain. Based on structural differences in the regulatory domain, PKCs are typically subdivided into three classes; conventional PKC (α, βI, βII, and γ subtypes), novel PKC (δ, ε, η, and θ subtypes), and atypical PKC (ζ and λ/ι subtypes). Conventional and novel PKCs have two types of membrane targeting domains, a tandem repeat of C1 domains (C1A and C1B), and a C2 domain, in the regulatory domain. The C1 domain (~50 residues) is a cysteine-rich compact structure that was identified as the interaction site for *sn*-1,2-diacylglycerol (DAG) and phorbol ester (4, 5). The C2 domain (~130 residues) is an eight-stranded β sandwich protein that is involved in Ca^{2+}-dependent membrane binding for conventional isoforms (6–8). All novel PKCs contain a Ca^{2+}-independent C2 domain in the amino terminus, followed by the C1A and C1B domains in the regulatory domain (see Fig. 1).

PKCε is a novel PKC expressed in many tissues and cells, but found abundantly in hormonal, immune, and neuronal cells (9). PKCε has been implicated in oncogenesis, antiviral resistance, hormone secretion, muscle contraction, mechanical force contraction, cardiac preconditioning, and diabetes (9). Additionally, key roles of PKCε have been established in numerous cellular processes, including differentiation, growth, gene expression, metabolism, transport, endocytosis, exocytosis, and regulation of transporters (9). In some mammalian cells, PKCε has been reported to have opposing functions to another novel PKC, PKCδ (10–12).

Although some specific PKCε substrates have been identified, such as calsequestrin (13) and the capsaicin receptor (14), most PKCε substrates, such as myristoylated alanine-rich C kinase substrate (15), are also phosphorylated by other conventional and novel PKCs. Thus, diverse cellular functions of PKCε should depend greatly on its exquisite subcellular targeting and activation. For this reason, the mechanism by which this PKC is targeted to a specific cell membrane and activated has been extensively studied. It has been reported (9) that the

* This work was supported by National Institutes of Health Grants GM52598, GM53987, and GM68849. The costs of publication of this article were defrayed in part by the payment of page charges. This article must therefore be hereby marked "*advertisement*" in accordance with 18 U.S.C. Section 1734 solely to indicate this fact.

‡ Present address: Laboratory of Fluorescence Dynamics, Dept. of Physics, University of Illinois Urbana-Champaign, 1110 West Green St., Urbana, IL 61801-63080.

§ Present address: Dept. of Cell Biology, Yale University School of Medicine, P. O. Box 208002, 333 Cedar St., New Haven, CT 06520-8002.

¶ Present address: Dept. of Pharmacology and Molecular Sciences, Johns Hopkins University, Baltimore, MD 21205.

‖ To whom correspondence should be addressed: Dept. of Chemistry (M/C 111), University of Illinois at Chicago, 845 West Taylor St., Chicago, IL 60607-7061. Tel.: 312-996-4883; Fax: 312-996-2183; E-mail: wcho@uic.edu.

[1] The abbreviations used are: PKC, protein kinase C; CHAPS, (3-[3-cholamidopropyl)dimethylammonio]-1-propane-sulfonate DAG, *sn*-1,2-diacylglycerol; OPG, 1-octanoyl-2-(8-pyrenyloctanoyl)-*sn*-3-glycerol; DiC_8, *sn*-1,2-dioctanoylglycerol; DiC_{18}, *sn*-1,2-dioleoylglycerol; DMEM, Dulbecco's modified eagles medium; EGFP, enhanced green fluorescent protein; FBS, fetal bovine serum; HEK, human embryonic kidney; PMA, phorbol 12-myristate 13-acetate; POPC, 1-palmitoyl-2-oleoyl-*sn*-glycero-3-phosphocholine; POPE, 1-palmitoyl-2-oleoyl-*sn*-glycero-3-phosphoethanolamine; POPG, 1-palmitoyl-2-oleoyl-*sn*-glycero-3-phosphoglycerol; POPI, 1-palmitoyl-2-oleoyl-*sn*-glycero-3-phosphoinositol; POPS, 1-palmitoyl-2-oleoyl-*sn*-glycero-3-phosphoserine; PS, phosphatidylserine; SPR, surface plasmon resonance; OPG, 1-octanoyl-2-(8-pyrenenyloctanoyl)-sn-glycerol.

membrane targeting and activation of PKCϵ is regulated by phosphorylation, DAG and other lipids, and adaptor proteins. Phosphorylation of PKCs on the canonical sites in the activation loop, turn motif, and hydrophobic motif, respectively, by either upstream protein kinases or autophosphorylation has been proposed to be essential for enzyme activity and stability (1, 16). PKCϵ also has activation loop, turn, and hydrophobic motif sites at Thr^{566}, Thr^{710}, and Ser^{729}, respectively.

As with other conventional and novel PKCs, the membrane targeting and activation of PKCϵ is mediated by DAG. In addition, it was reported (17) that arachidonic acid and ceramide could induce the translocation of PKCϵ to the Golgi complex by interacting with its C1B domain. The subcellular localization of PKCϵ also seems to be influenced by adaptor proteins. Several reports have indicated that PKCϵ interacts with the Golgi membrane coatmer protein β′-COP (RACK2 or ϵRACK) (18) via its C2 domain and actin (19) through an actin-binding motif located between the C1A and C1B domains.

Despite these studies, the mechanism of PKCϵ activation by DAG is not fully understood. We have recently performed a series of investigations on the mechanisms of membrane targeting and activation of conventional PKCs (PKCα and PKCγ) (20–22) and a novel PKC (PKCδ) (23), with a particular emphasis on elucidating the roles of C1A, C1B, and C2 domains in these processes. These studies have revealed that individual PKC isoforms follow distinct activation mechanisms due in part to the differences in the conformational flexibility and DAG affinity of their C1 domains. It has been also recognized that some PKCs, such as PKCα and PKCδ, are activated by DAG and phorbol esters through different mechanisms, because their C1A and C1B domains have opposite relative affinities for these ligands (22). As continuation of this line of investigation, we studied how DAG induces the cellular membrane translocation and activation of PKCϵ. Extensive *in vitro* lipid binding studies and cellular membrane translocation measurements of PKCϵ and mutants, as well as its isolated C1A, C1B, and C2 domains, by means of isothermal titration calorimetry, surface plasmon resonance (SPR), monolayer penetration analyses, and two-photon microscopy, respectively, reveal that PKCϵ has a distinctly different membrane binding and activation mechanism than PKCδ, which derives from comparably high DAG affinity and conformational flexibility of the two C1 domains of PKCϵ.

EXPERIMENTAL PROCEDURES

Materials—1-Palmitoyl-2-oleoyl-*sn*-glycero-3-phosphatidic acid (POPA), 1-Palmitoyl-2-oleoyl-*sn*-glycero-3-phosphocholine (POPC), 1-palmitoyl-2-oleoyl-*sn*-glycero-3-phosphoethanolamine (POPE), 1-palmitoyl-2-oleoyl-*sn*-glycero-3-phosphoglycerol (POPG), 1-palmitoyl-2-oleoyl-*sn*-glycero-3-phosphoinositol (POPI), 1-palmitoyl-2-oleoyl-*sn*-glycero-3-phosphoserine (POPS), *sn*-1,2-dioctanoylglycerol (DiC_8), and *sn*-1,2-dioleoylglycerol (DiC_{18}) were purchased from Avanti Polar Lipids, Inc. (Alabaster, AL) and used without further purification. Phorbol 12,13-dibutyrate, phorbol 12-myristate-13-acetate (PMA), cholesterol, fatty acid-free bovine serum albumin, Triton X-100, ATP, octylglucoside, and CHAPS were from Sigma. Phospholipids concentrations were determined by a modified Bartlett analysis (24). [γ-^{32}P]ATP (3 Ci/μmol) was from Amersham Biosciences. Restriction endonucleases and enzymes for molecular biology were obtained from New England Biolabs (Beverly, MA). Pioneer L1 sensor chip was from Biacore AB (Piscataway, NJ). Dulbecco's modified Eagle's medium (DMEM) and Lipofectamine™ were from Invitrogen. Human embryonic kidney (HEK) 293 cell line, Zeocin, and ponasterone A were from Invitrogen.

Synthesis of OPG—A fluorescent DAG analog, OPG, was synthesized from L-2,3-*O*-isopropyliden-*sn*-glycerol (Aldrich) by a multistep synthesis. First, octanoyl chloride (1.34 g, 8.3 mmol) and triethylamine (1.2 ml, 8.3 mmol) were added to a stirred solution of L-2,3-*O*-isopropyliden-*sn*-glycerol (1 g, 7.5 mmol) in dry dichloromethane (20 ml) under N_2 atmosphere at 0 °C. The reaction mixture was warmed to room temperature and stirred at 23 °C for 24 h. The reaction was quenched with saturated sodium bicarbonate solution and extracted with dichloromethane. The organic layer was dried over anhydrous Na_2SO_4. Evaporation of solvent under reduced pressure resulted in an oily mixture, which was purified by flash silica gel chromatography (20% ethyl acetate/hexane) to yield (2,2-dimethyl-1,3-dioxolan-4-yl)methyl octanoate. This compound (1.2 g) in 90% methanol (30 ml) was refluxed for 16 h in the presence of DOWEX 50WX8(H^+) resin (Sigma). The reaction mixture was cooled down, and solvent was removed under reduced pressure. The mixture was extracted with ethyl acetate. Evaporation of solvent under reduced pressure afforded 2,3-dihydroxypropyl octanoate, which was used without further purification. To a stirred solution of 2,3-dihydroxypropyl octanoate (0.52 g, 2.8 mmol) in dry dichloromethane under N_2 atmosphere at 0 °C, were added trityl chloride (0.93 g, 3.35 mmol), pyridine (0.35 ml, 3.35 ml), and 4-(dimethylamino)pyridine (catalytic amount). After stirring at room temperature for 14 h, the reaction mixture was washed with saturated sodium bicarbonate solution. The organic layer was dried over anhydrous Na_2SO_4. Evaporation of solvent under reduced pressure resulted in a solid mixture, which was purified by flash silica gel chromatography (10% ethyl acetate/hexane) to afford 2-hydroxy-3-(trityloxy)propyl octanoate as a major product. Separately, 8-pyrenyloctanoic acid was synthesized from sebacic acid and pyrene as described previously (25) and was converted to acid chloride by treating with 1.5 M equivalent of oxalyl chloride in dichloromethane at 0 °C for 2 h. To a stirred solution of 8-pyrenyloctanoyl chloride (0.2 g, 0.5 mmol) in dry dichloromethane under N_2 atmosphere at 0 °C, were added 2-hydroxy-3-(trityloxy)propyl octanoate (0.1 g, 0.23 mmol) and triethylamine (0.2 ml, 1.5 mmol). After stirring at 23 °C for 28 h the reaction mixture was washed with saturated ammonium chloride. After removing solvent under reduced pressure the crude mixture was stirred at 23 °C with Amberlyst 15-H in methanol for 1 h to remove the trityl group. The reaction mixture was filtered and solvent was removed under reduced pressure to afford OPG, which was purified by flash silica gel chromatography (10% ethyl acetate/hexane).

Expression Vector Construction and Mutagenesis—Expression vectors for the C1A and C1B domains were constructed by subcloning the C1A and C1B domain sequences of rat PKCϵ into pET21d vectors (Novagen, Madison, WI) between NcoI and XhoI sites by overlap extension PCR (26) using *Pfu* polymerase (Stratagene, La Jolla, CA). The C2 domain of PKCϵ was subcloned between NdeI and XhoI sites in pET28a. These vectors were designed to introduce an amino-terminal His_6 tag that can be removed by thrombin after affinity purification. Baculovirus transfer vectors encoding the cDNA of PKCϵ with appropriate C1 domain mutations were generated by the overlap extension PCR using pVL1392-PKC-ϵ plasmid as a template (27). The PCR product was purified on an agarose gel, and the PKCϵ gene was digested with NotI and BglII and subcloned into the pVL1392 vector. The mutagenesis was verified by DNA sequencing. Mammalian expression vectors for PKCϵ and mutants with carboxyl-terminal enhanced green fluorescence protein (EGFP) tags were generated by subcloning the respective genes into the pIND (Invitrogen) with the spacer sequence, GGNSGG, as described previously (23). Expression vectors for PKCϵ and PKCδ containing a carboxyl-terminal *Heteractis crispa* far-red fluorescent protein (HcRed; Clontech) tag were generated in the same fashion.

Protein Expression and Purification—*Escherichia coli* strain BL21(DE3) (Novagen) was used as a host for C1 domain expression. The C2 and C1B domains were expressed as soluble proteins, whereas the C1A domain formed inclusion bodies. These isolated domains were expressed and purified as previously described (22, 28). Full-length PKCϵ and mutants were expressed in baculovirus-infected Sf9 cells. The transfection of Sf9 cells with pVL1392-PKCϵ constructs was performed using a BaculoGold™ transfection kit from BD Pharmingen. The plasmid DNA for transfection was prepared by using an EndoFree Plasmid Maxi kit (Qiagen) to avoid potential endotoxin contamination. Cells were incubated for 4 days at 27 °C, and the supernatant was collected and used to infect more cells for the amplification of virus. After three cycles of amplification, high titer virus stock solution was obtained. Sf9 cells were maintained as monolayer cultures in TMN-FH medium (Invitrogen) containing 10% fetal bovine serum (Invitrogen). For protein expression, cells were grown to 2×10^6 cells/ml in 350-ml suspension cultures and infected with the multiplicity of infection of 10. The cells were then incubated for 60 h at 27 °C. PKCϵ wild type and mutants were purified as described previously (27).

Determination of PKC Activity—Activity of PKCϵ was assayed at 23 °C by measuring the initial rate of [^{32}P]phosphate incorporation from [γ-^{32}P]ATP (50 μM, 0.6 μCi/tube) into myelin basic protein (200 μg/ml) (Sigma). The reaction mixture contained large unilamellar vesicles (0.2 mM total lipid concentration), 0.16 M KCl, and 5 mM $MgCl_2$ in 20 mM HEPES, pH 7.4. Control experiments were done in the same

manner except buffer was used to replace the lipid vesicles to determine the background activity of PKCε. Reaction was started by adding 50 mM $MgCl_2$ to the mixture and incubating for 10 min at room temperature, and quenched by addition of 50 μl of 5% phosphoric acid. Seventy-five microliters of quenched reaction mixtures were spotted on P-81 ion-exchange paper, washed four times with a 5% solution of phosphoric acid, followed by one wash in 95% ethanol. Papers were transferred into scintillation vials containing 4 ml of scintillation fluid (Fisher Scientific), and radioactivity was measured by liquid scintillation counting.

Monolayer Measurements—Surface pressure (π) of solution in a circular Teflon trough (4-cm diameter × 1-cm deep) was measured using a Wilhelmy plate attached to a computer-controlled Cahn electrobalance (Model C-32) as described previously (27). All experiments were done at 23 °C, where 5–10 μl of phospholipid solution in ethanol/hexane (1:9 (v/v)) was spread onto 10 ml of subphase (20 mM Tris-HCl, pH 7.4, containing 0.16 M KCl) to form a monolayer with a given initial surface pressure (π_0). The subphase was continuously stirred at 60 rpm with a magnetic stir bar. Once the surface pressure reading of monolayer had been stabilized (after ~5 min), the protein solution (typically 60 μl) was injected into the subphase through a small hole drilled at an angle through the wall of the trough, and the change in surface pressure (D_p) was measured as a function of time. Typically, the $\Delta\pi$ value reached a maximum after 30 min. The maximal $\Delta\pi$ value at a given π_0 depended on the protein concentration and reached a saturation value. Protein concentrations in the subphase were therefore maintained above such values to ensure that the observed $\Delta\pi$ represented a maximal value (20 μg of total of PKCε and mutants). The critical surface pressure (π_c) was determined by extrapolating the $\Delta\pi$ versus π_0 plot to the *x*-axis (29).

Surface Plasmon Resonance Analysis—Kinetics of vesicle-protein binding was determined by the SPR analysis using a BIAcore X biosensor system (Biacore AB) and the L1 chip as described previously (23, 30). The first flow cell was used as a control cell and was coated with 5000 RU of POPC. The second flow cell contained the surface coated with vesicles with varying lipid compositions (*e.g.* POPC/POPS/DiC_{18} = 59:40:1) at 5000 resonance units. After lipid coating, 30 μl of 50 mM NaOH was injected at 100 μl/min three times to wash out unbound lipids and stabilize the lipid layer. Typically, no further decrease in SPR signal was observed after one wash cycle. After coating, the drift in signal was allowed to stabilize below 0.3 resonance unit/min before any binding measurements, which were performed at 23 °C and a flow rate of 30 μl/min. 90 μl of protein sample was injected for an association time of 3 min while the dissociation was then monitored for 10 min in running buffer. After each measurement, the lipid surface was typically regenerated with a 10-μl pulse of 50 mM NaOH. The regeneration solution was passed over the immobilized vesicle surface until the SPR signal reached the initial background value before protein injection. For data acquisition, five or more different concentrations (typically within a 10-fold range above or below the K_d) of each enzyme were used, and data sets were repeated three or more times. When needed, the entire lipid surface was removed with a 5-min injection of 40 mM CHAPS followed by a 5-min injection of 40 mM octylglucoside at 5 μl/min, and the sensor chip was recoated for the next set of measurements. All data were analyzed using BIAevaluation 3.0 software (Biacore) to determine the rate constants of association (k_a) and dissociation (k_d) as described previously (23, 30). Equilibrium dissociation constant (K_d) was either calculated from rate constants using an equation, $K_d = k_d/k_a$ assuming 1:1 binding, or directly determined from steady-state binding measurements as described previously (22). Mass transport was not a limiting factor in our experiments, as change in flow rate or ligand density did not affect kinetics of association and dissociation.

Isothermal Titration Calorimetry Measurements—Binding of C1 domains to water-soluble phorbol 12,13-dibutyrate or DiC_8 ligands was measured using a MicroCal VP isothermal titration calorimeter (MicroCal Inc., Northampton, MA) as described previously (22). Protein samples used for the titration were prepared by dialyzing overnight against 4 liters of a working buffer (20 mM Tris-HCl, pH 7.0, 50 μM $ZnSO_4$). Measurements were performed at 30 °C using the working buffer as a reference and a diluent. Protein concentration was 35 nM, whereas ligand concentration used for each measurement varied according to the range of K_d value to be determined (*e.g.* 0–1 μM for 10 nM K_d; see Table II). Binding measurements were performed with 5-μl stepwise injections of the ligand into the protein in the sample cell. Injections were continued until saturating signals were obtained. The collected data were analyzed with the Origin software (MicroCal) using a simple single-site model.

Cell Culture—A stable HEK 293 cell line expressing the Ecdysone receptor (Invitrogen) was used for all experiments (31). Cells were cultured in DMEM supplemented with 10% fetal bovine serum at 37 °C in 5% CO_2 and 98% humidity until 90% confluent. Cells were then passaged into 8 wells of a Lab-Tech™ chambered coverglass for later transfection and visualization. Only cells between the 5th and 20th passages were used. For transfection, 80–90% confluent cells in Lab-Tech™ chambered coverglass wells were exposed to 150 μl of unsupplemented DMEM containing 0.5 μg of endotoxin-free DNA and 1 μl of Lipofectamine reagent for 7–8 h at 37 °C. After exposure, the transfection medium was removed, and the cells were washed once with fetal bovine serum-supplemented DMEM and overlaid with fetal bovine serum-supplemented DMEM containing Zeocin and 5 μg/ml ponasterone A to induce protein production for 16–24 h.

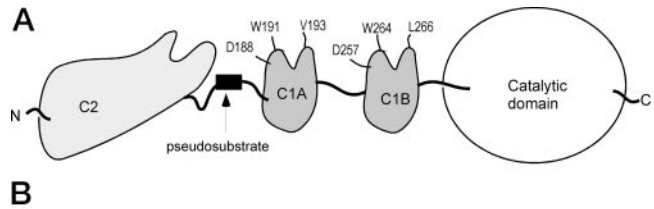

FIG. 1. **A schematic domain structure of PKCε (*A*) and the amino acid sequence alignment of C1 domains of PKCδ and PKCε (*B*).** Novel PKCs have an amino-terminal Ca^{2+}-independent C2 domain connected to a tandem repeat of C1 domains (C1A and C1B) that are in turn connected to a carboxyl-terminal catalytic domain. A pseudosubstrate sequence is located between the C2 and C1A domain. Mutated hydrophobic residues and anionic residues in the C1 domains are illustrated in the *schematic* (*A*) and also shown in *bold-faced characters* in the sequence (*B*).

Microscopy—Microscopy data were collected on a custom-built combination laser scanning confocal and multiphoton microscope as described previously (23). All experiments were carried out at the same laser power and gains and offset setting on the photomultiplier tubes. Transfected cells were washed twice with HEK buffer (1 mM HEPES, pH 7.4, containing 2.5 mM $MgCl_2$, 140 mM NaCl, 5 mM KCl, and 6 mM sucrose). After washing, cells were overlaid with 150 μl of HEK buffer. Suitable cells were selected for imaging, and a single image was taken for each cell before addition of OPG or DiC_8. Then, the translocation of protein and subcellular localization of lipid was simultaneously monitored at fixed intervals (every 7 s) after 150 μl of HEK buffer containing 0.1 mg/ml OPG (or DiC_8) was added. Control experiments were done with Me_2SO. Images were analyzed using simFCS. Specifically, regions of interest in the cytosol were defined, and the average intensity in a square (1 × 1 μm) obtained with respect to time. Membrane intensities were determined for each frame in individual cells by extending a line from cytosol to the outside of the cell and reading off the intensity with distance along the line. Intensity values corresponding to the place on the line indicating the edge of the cell were averaged. Lines were drawn in at least three places in each cell, and membrane intensity was determined. These values were averaged, and the resultant cytosolic intensity values were converted to a ratio for each frame: membrane/(membrane + cytosol). The values were then scaled for the entire time series from 0% to 100% of the obtained ratio for a given experiment. This allowed a comparison of ratiometric changes between experiments. Note that each experiment was repeated at least three times on a given day and was repeated at least two different days with different transfected cells.

RESULTS

PS-independent Membrane Binding and Activation of PKCε—Despite the long-held notion that phosphatidylserine (PS) greatly enhances the membrane affinity and activity of PKCs (32), our recent studies have revealed that the PS dependence can vary significantly among PKC isoforms (22, 27). Among conventional PKCs, PKCα (27) and $PKC\beta_{II}$ (33) strongly prefer PS to other anionic phospholipids, such as phosphatidylglycerol (PG), whereas PKCγ shows little selectivity for PS over PG (22). Among novel PKCs, PKCδ shows a high degree of PS selectivity (23), whereas PKCε does not display significant PS selectivity (27). Our studies have also indicated that the PS selectivity of PKCα (20) and PKCδ (23) is ascribed to the

TABLE I
Membrane binding parameters for PKCε and mutants determined from SPR analysis

Values represent the mean and standard deviation from five determinations. All measurements were performed in 10 mM HEPES, pH 7.4, containing 0.16 M KCl.

Proteins	k_a	k_d	K_d[a]	Increase in K_d[b]
	$M^{-1}\ s^{-1}$	s^{-1}	M	
POPC/POPS/DiC_{18} (59:40:1)				
PKCε	$(1.9 \pm 0.2) \times 10^5$	$(3.7 \pm 0.3) \times 10^{-4}$	$(2.0 \pm 0.3) \times 10^{-9}$	
T35E	$(1.6 \pm 0.3) \times 10^5$	$(4.0 \pm 0.4) \times 10^{-4}$	$(2.5 \pm 0.5) \times 10^{-9}$	1.1
D188A	$(2.8 \pm 0.5) \times 10^5$	$(2.9 \pm 0.5) \times 10^{-4}$	$(1.0 \pm 0.2) \times 10^{-9}$	0.5
W191G	$(7.9 \pm 1.0) \times 10^4$	$(8.4 \pm 0.9) \times 10^{-4}$	$(1.1 \pm 0.2) \times 10^{-8}$	5
V193G	$(1.4 \pm 0.2) \times 10^5$	$(1.2 \pm 0.2) \times 10^{-3}$	$(8.6 \pm 2.0) \times 10^{-9}$	4
D257A	$(1.2 \pm 0.3) \times 10^5$	$(4.0 \pm 0.6) \times 10^{-4}$	$(3.3 \pm 1.0) \times 10^{-9}$	1.5
W264G	$(7.9 \pm 0.6) \times 10^4$	$(7.1 \pm 0.8) \times 10^{-4}$	$(9.0 \pm 1.0) \times 10^{-9}$	4
L266G	$(2.0 \pm 0.5) \times 10^5$	$(2.2 \pm 0.3) \times 10^{-3}$	$(1.0 \pm 0.3) \times 10^{-8}$	5
W191G/W264G	$(4.9 \pm 0.6) \times 10^4$	$(2.0 \pm 0.3) \times 10^{-3}$	$(4.1 \pm 0.8) \times 10^{-8}$	19
C2 deletion	$(3.2 \pm 0.6) \times 10^5$	$(4.5 \pm 0.4) \times 10^{-4}$	$(1.4 \pm 0.3) \times 10^{-9}$	0.6
POPC/POPG/DiC_{18} (59:40:1)				
PKCε	$(2.3 \pm 0.5) \times 10^5$	$(3.4 \pm 0.4) \times 10^{-4}$	$(1.5 \pm 0.4) \times 10^{-9}$	0.7
D188A	$(2.6 \pm 0.6) \times 10^5$	$(2.8 \pm 0.3) \times 10^{-4}$	$(1.1 \pm 0.3) \times 10^{-9}$	0.5
D257A	$(1.8 \pm 0.4) \times 10^5$	$(3.4 \pm 0.4) \times 10^{-4}$	$(1.9 \pm 0.5) \times 10^{-9}$	0.9
C2 deletion	$(3.6 \pm 0.5) \times 10^5$	$(2.8 \pm 0.3) \times 10^{-4}$	$(7.8 \pm 1.4) \times 10^{-10}$	0.4

[a] K_d determined by k_d/k_a for these measurements.
[b] The increase (-fold) in K_d relative to the binding of PKCε to POPC/POPS/DiC_{18} (59:40:1).

specific PS-induced unleashing of C1 domains that are tethered intramolecularly via highly conserved Asp or Glu (*e.g.* Glu^{177} of C1A and Asp^{245} of C1B for PKCδ; Fig. 1*B*). On the other hand, lack of PS selectivity of PKCγ is due to higher conformational flexibility of its C1 domains (22). To see if the PS-independent membrane binding and activation of PKCε is also due to the higher conformational flexibility of C1 domains, we characterized the membrane binding and activation of PKCε and its D188A and D257A mutants. Asp^{188} (C1A) and Asp^{257} (C1B) of PKCε correspond to Glu^{177} and Asp^{245} of PKCδ, respectively (see Fig. 1).

We first measured the binding of PKCε and the mutants to vesicles with different compositions by the SPR analysis, which has been shown to be a powerful tool for measuring membrane-protein interactions (29, 30, 34). In agreement with our previous report, PKCε exhibited similar affinity for POPC/POPS/DiC_{18} (59:40:1 in mole ratio) and POPC/POPG/DiC_{18} (59:40:1) vesicles (Table I). Also, D188A and D257A had comparable binding affinity for PS- and PG-containing vesicles. When the affinity for PS-containing vesicles was compared, D188A had modestly (*i.e.* 2-fold) higher affinity than wild type, whereas D257A had 50% lower affinity than wild type. These results are similar to those seen for PKCγ (22) but in sharp contrast to those reported for PKCα (20) and PKCδ (23). This similarity between PKCε and PKCγ suggests that PKCε also has conformationally flexible C1 domains.

To further test this notion, we measured the interactions of PKCε with various lipid monolayers at the air-water interface. We have shown for many PKC isoforms that hydrophobic residues near the DAG-binding pocket of the C1 domain are primarily responsible for the partial penetration of PKCs to lipid monolayers (20, 22, 23). Accordingly, PS specifically enhanced the monolayer penetration of PKCα and PKCδ with conformationally restricted C1 domains, whereas it had no such effect on PKCγ with conformationally flexible C1 domains. In this study, we monitored $\Delta\pi$ caused by the penetration of PKCε to POPC/POPS and POPC/POPG mixed monolayers with varying surface packing density (*i.e.* different π_0). DAG was not included in the monolayer, because it has been shown to have no effect on the monolayer penetration *per se* of PKCε and other PKCs, albeit greatly enhancing its membrane affinity (27, 35). The resulting $\Delta\pi$ *versus* π_0 plots (Fig. 2) show that PKCε can penetrate PS- and PG-containing monolayers equally well, which is in sharp contrast to PKCδ that showed PS-dependent monolayer penetration (23). This, in conjunction with the fact that the PS-independent monolayer penetration of PKCε is comparable to the PS-dependent monolayer penetration of PKCδ, is consistent with the notion that C1 domains of PKCε are not conformationally restricted. Also, D188A and D257A showed wild type-like monolayer penetration (Fig. 2).

We then measured the kinase activity of PKCε, D188A, and D257A in the presence of PS- and PG-containing vesicles, *i.e.* POPC/POPS(G)/DiC_{18} ((99 − *x*):*x*:1). Fig. 3 clearly shows that all these proteins are activated similarly by PS- and PG-containing vesicles. Collectively, these results indicate that PS-independent membrane binding and activity of PKCε is due to the high conformational flexibility and ready accessibility of its C1 domains.

DAG Affinity of C1A and C1B Domains and Their Roles in PKCε Activation—We previously measured the DAG affinities of isolated C1 domains of several PKCs by isothermal titration calorimetry analysis, which indicated that differential roles of C1A and C1B domains in the membrane targeting and activation of PKCs are ascribed to their different DAG affinities (22, 23). For PKCα (20, 22) and PKCδ (23) whose C1A domain has much higher DAG affinity than C1B domain, the C1A domain plays a predominant role in these processes, whereas for PKCγ whose C1A and C1B domains have comparable DAG affinities, both C1 domains participate in the processes (22). To see how the C1A and C1B domains of PKCε are involved in its membrane binding and activation, we first expressed the isolated C1A and C1B domains of PKCε. The C1B domain was expressed as a soluble protein in *E. coli*, whereas the C1A domain was expressed as inclusion bodies, which were then solubilized in urea and refolded.

We first determined by isothermal titration calorimetry analysis the affinity of the C1A and C1B domains for a short-chain DAG analog, DiC_8, which was shown to exist as a monomer in the concentration range (10–100 nM) used for this binding study as its critical micellar concentration is ~15 μM (22). As shown in Table II, both C1 domains showed relatively high affinity for DiC_8, although the C1A domain has ~3-fold higher affinity (K_d = 38 nM) than the C1B domain (K_d = 110 nM). This difference is much smaller than the affinity difference between the two C1 domains seen for PKCδ and PKCα (>100-fold) but larger than that reported for PKCγ (only 20% difference) (22). We then measured the affinity of PKCε C1 domains for a short-chain phorbol ester phorbol 12,13-dibutyrate. The

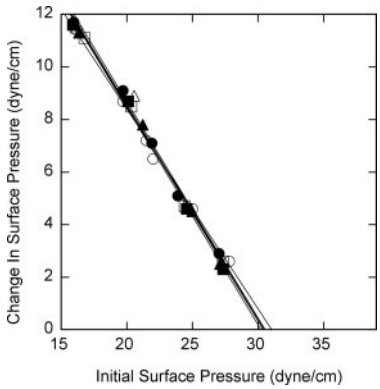

FIG. 2. **Monolayer penetration of PKCε and C1 domain anionic site mutants.** PKCε wild type (*circles*), D188A (*triangles*), and D257A (*squares*) were used with POPC/POPS (7:3) (*open symbols*) and POPC/POPG (7:3) monolayers (*filled symbols*). The subphase was 20 mM Tris buffer, pH 7.4, containing 0.16 M KCl.

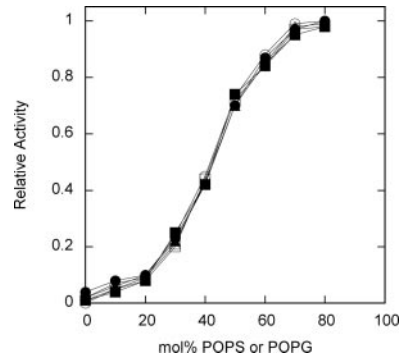

FIG. 3. **Enzymatic activity of PKCε and C1 domain anionic site mutants in the presence of POPC/POPS(G)/DiC$_{18}$ vesicles.** Wild type (*circles*), D188A (*triangles*), and D257A (*squares*) were used with POPC/POPS/DiC$_{18}$ (99 − *x*:*x*:1) (*open symbols*) and POPC/POPG/DiC$_{18}$ (99 − *x*:*x*:1) (*filled symbols*) vesicles in 20 mM HEPES buffer, pH 7.4, containing 0.16 M KCl, 5 mM $MgCl_2$, and myelin basic protein (200 μg/ml). Each data point represents an average of duplicate measurements. Relative activity was calculated in comparison with the maximal activity of wild type achieved with PS vesicles.

C1A and C1B domains have the K_d values of 74 and 23 nM, respectively. This is consistent with a previous report showing that the C1B domain has 7-fold higher affinity for phorbol 12,13-dibutyrate than the C1A domain (36), thereby verifying that the C1A and C1B domains of PKCε were correctly folded. Also, these data are in line with the reported trend that C1A and C1B domains of PKCs have opposite relative affinities for DAG and phorbol esters (37, 38): *i.e.* C1A has higher affinity for DAG, whereas the C1B has higher affinity for phorbol ester.

We also measured by the SPR analysis the binding of C1A and C1B domains to DAG (DiC$_{18}$) and phorbol ester (PMA) with longer acyl chains that were incorporated in the lipid bilayer. The C1A and C1B domains had the K_d values of 11 and 52 nM, respectively, for the POPC/POPS/DiC$_{18}$ (67.5:30:2.5) vesicles, whereas having the K_d values of 14 and 5.2 nM for POPC/POPS/PMA (69.95:30:0.05) vesicles (notice that these K_d values are not for DiC$_{18}$ or PMA but for vesicles containing these lipids). This underscores that C1A and C1B domains of PKCε have relatively high affinities for both soluble and membrane-incorporated DAG and phorbol esters. Relatively high DAG affinities of the two C1 domains of PKCε, as well as their high conformational flexibility, suggest that both C1 domains might play a role in the DAG-mediated membrane binding and activation of PKCε.

To test this notion, we measured the effects of selected mutations of the C1A and C1B domains of PKCε on its membrane binding and activation by the SPR analysis. Mutations were made on the hydrophobic residues whose counterparts in conventional PKCs and PKCδ have been shown to be important for their membrane binding (20, 22); *i.e.* W191G and V193G for the C1A domain and W264G and L266G for the C1B domain (see Fig. 1). As shown in Table I, all four mutants showed 4- to 5-fold lower affinity than wild type for POPC/POPS/DiC$_{18}$ (59:40:1) vesicles. All the mutants had larger k_d values than wild type, which is consistent with the notion that the mutated hydrophobic residues are involved in membrane penetration (30). Monolayer measurements further supported this notion, because all the mutations reduced penetration into the POPC/POPS (5:5) monolayer to similar extents (Fig. 4). A double-site mutant, W191G/W264G, had 19-times lower affinity than wild type for POPC/POPS/DiC$_{18}$ (59:40:1) vesicles and showed significantly more reduced monolayer penetration than all single-site mutants. This indicates that the membrane binding of C1A and C1B domains is more additive than synergistic.

We then measured the kinase activities of these mutants in the presence of POPC/POPS/DiC$_{18}$ (100 − *x*:*x*:1) vesicles. With PS concentration < 40 mol%, both C1A (W191G and V193G) and C1B (W252G and L254G) domain mutants showed much lower activity than the wild type, underscoring the importance of both domains in enzyme activation (Fig. 5). Interestingly, the C1B domain mutants regained the wild type activity at higher PS concentration, whereas the C1A domain mutants had only ~20% of the wild type activity even at 80 mol% PS (Fig. 5). This indicates that the loss of membrane penetration and resulting hydrophobic interactions can be compensated for by strong electrostatic interactions for the C1B domain but not for the C1A domain in the activation of PKCε. These data suggest that, although both C1A and C1B domains contribute to the DAG-dependent membrane binding of PKCε, the membrane penetration of the C1A domain is more critical for optimal activation (*i.e.* removal of the pseudosubstrate from the active site) of this novel PKC due to the proximity between the C1A domain and the pseudosubstrate (see Fig. 1).

Role of C2 Domain in Membrane Binding and Activation of PKCε—It has been well established that the C2 domains of conventional PKCs are involved in the Ca^{2+}-dependent membrane binding and activation of these PKCs (6, 39, 40). However, the role of Ca^{2+}-independent C2 domains of novel PKCs still remains unclear. Our recent study indicated that the C2 domain of PKCδ did not contribute to the membrane binding and activation both *in vitro* and in the cell (23). The C2 domain of PKCε shares only 16% homology with that of PKCδ and major differences are found in their tertiary structures, particularly in the loop regions (41, 42). Also, recent studies have indicated that the C2 domain of PKCε may be involved in membrane binding. For instance, Ochoa *et al.* (42) reported that the C2 domain of PKCε could interact nonspecifically with anionic phospholipids, whereas Pepio *et al.* (43) reported that phosphorylation of Ser^{36} in the C2 domain of PKC *Aplysia* II, which is more closely related to mammalian PKCε/η than to PKCδ/θ, promoted the membrane interaction of the C2 domain. It was also suggested that the phosphatidic acid binding affinity of the PKCε C2 domain could enhance the translocation of PKCε to the membrane in RBL-2H3 cells (44).

To see if the C2 domain plays any role in the membrane binding and activation of PKCε, we measured the membrane binding properties of isolated C2 domain of PKCε and also measured the effect of C2 domain deletion on the membrane binding and activation of full-length PKCε. The isolated C2 domain of PKCε showed some affinity for anionic vesicles, including POPC/POPA (7:3) (K_d ~ 250 nM), POPC/POPS (7:3) (K_d ~ 500 nM), and POPC/POPG (7:3) (K_d ~ 500 nM) vesicles,

TABLE II

Phorbol ester binding parameters for PKCε C1 domains determined from ITC and SPR analyses

Values represent the mean and standard deviation from three determinations. All measurements were performed in 10 mM HEPES, pH 7.4, containing 0.16 M KCl unless specified otherwise.

Proteins	PDBu (literature)[a]	PDBu (ITC analysis)		PMA (SPR analysis)[b]	DiC_8 (ITC analysis)		DiC_{18} (SPR analysis)[c]
	K_d	Stoichiometry	K_d	K_d[d]	Stoichiometry	K_d	K_d[d]
	nM		*nM*	*nM*		*nM*	*nM*
PKCε-C1A	5.6	0.90 ± 0.02	74 ± 10	14 ± 3	0.90 ± 0.01	38 ± 5	11 ± 1
PKCε-C1B	0.81	1.10 ± 0.01	23 ± 9	5.2 ± 1	1.00 ± 0.01	110 ± 40	52 ± 10
PKCδ-C1A[e]	~300	NM[f]	NM	360 ± 21	0.91 ± 0.05	85 ± 27	30 ± 2
PKCδ-C1B[e]	1.0 ± 0.1	0.96 ± 0.01	58 ± 26	40 ± 4	NM[f]	NM	7800 ± 1800

[a] Taken from Ref. 36.
[b] POPC/POPS/PMA (69.95:30:0.05) vesicles.
[c] POPC/POPS/DiC_{18} (67.5:30:2.5) vesicles.
[d] K_d determined from equilibrium analysis for these measurements. Notice that K_d determined from SPR measurements is the dissociation constant not for DAG (or phorbol ester) but for DAG (or phorbol ester)-containing vesicles.
[e] Taken from Ref. 23.
[f] NM, not measurable.

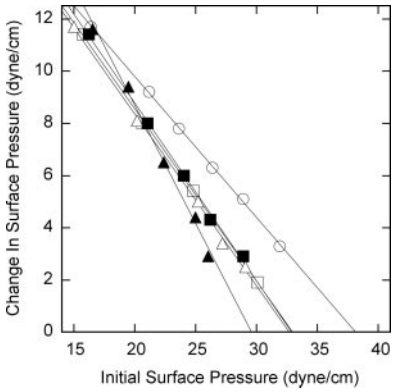

FIG. 4. **Monolayer penetration of PKCε and C1 domain hydrophobic site mutants.** $\Delta\pi$ was measured as a function of π_0 for PKCε wild type (○), W191G (□), V193G (■), W264G (△), and W191G/W264G (▲) with the POPC/POPS (5:5) monolayer. The subphase was 20 mM Tris buffer, pH 7.4 containing 0.16 M KCl.

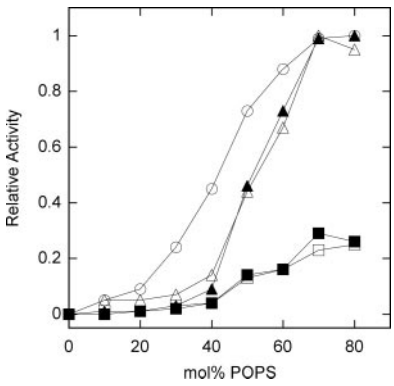

FIG. 5. **Enzymatic activity of PKCε and C1 domain hydrophobic site mutants in the presence of POPC/POPS/DiC_{18} vesicles.** Wild type (○), W191G (□), V193G (■), W264G (△), and L266G (▲) were employed with POPC/POPS/DiC_{18} (99 − *x*:*x*:1) vesicles. Experimental conditions were the same as described for Fig. 3.

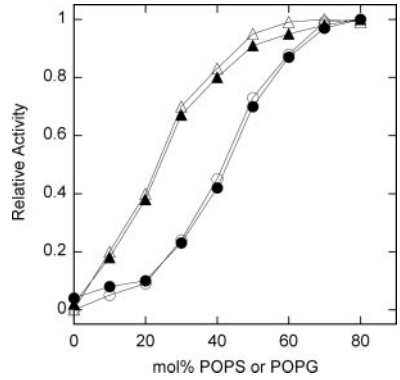

FIG. 6. **Enzymatic activity of PKCε and C2 deletion mutant in the presence of POPC/POPS(G)/DiC_{18} vesicles.** The kinase activity of 30 nM of PKCε (*circles*) and its C2 deletion mutant (*triangles*) was measured in the presence of 0.2 mM of POPC/POPS/DiC_{18} (99 − *x*:*x*:1) (*open symbols*) or POPC/POPG/DiC_{18} (99 − *x*:*x*:1) (*filled symbols*) vesicles. Experimental conditions were the same as described for Fig. 3.

but this binding is much weaker than that of the full-length PKCε (K_d ~ 2 nM) for these vesicles. This indicates that the C2 domain alone would not contribute much to the overall binding of PKCε. To see if the phosphorylation of the C2 domain enhances the membrane affinity, we measured the vesicle binding of a phosphorylation mimic mutant of PKCε (T35E). Thr^{35} of PKCε corresponds to Ser^{36} of Aplysia II PKC. As shown in Table I, T35E of PKCε behaved similarly to the wild type, suggesting that the membrane affinity of the C2 domain of PKCε is not enhanced by phosphorylation. Also, the isolated C2 domain carrying the T35E mutation had essentially the same affinity for POPC/POPS (7:3) (K_d ~ 520 nM) as the wild type C2 domain. When we measured the vesicle binding affinity and enzyme activity of C2 deletion construct (ΔC2), no significant negative effect by the deletion was observed. Instead, ΔC2 had slightly (~60%) higher affinity for POPC/POPS/DiC_{18} (59:40:1) vesicles (Table I) and slightly higher (<50%) activity (Fig. 6) than PKCε wild type. Collectively, these data indicate that the C2 domain does not significantly contribute to the membrane binding and activation of PKCε.

Cellular Membrane Translocation—To understand how *in vitro* membrane binding properties of PKCε affect its cellular membrane targeting, we monitored the DAG-dependent subcellular translocation of PKCε and selected mutants, each tagged with EGFP at their carboxyl termini, in HEK293 cells. Control SPR experiments showed that PKCε with the EGFP tag at the carboxyl terminus had the affinity for POPC/POPS/DiC_{18} (59:40:1) vesicles that was comparable to their non-EGFP tagged counterparts employed in *in vitro* studies (*e.g.* K_d = 2.5 ± 0.5 nM for wild type PKCε-EFGP). Furthermore, the cellular level of expression of different protein constructs was comparable in most cells (>90%), when assessed by visual inspection of EGFP fluorescence intensity and by Western blotting using PKCε-specific antibodies (data not shown). Only those cells with similar PKCε expression levels were used for further measurements.

We simultaneously monitored by two-photon microscopy the spatiotemporal dynamics of EGFP-tagged PKCε and a short-chain fluorogenic DAG, OPG (0.1 mg/ml). We previously

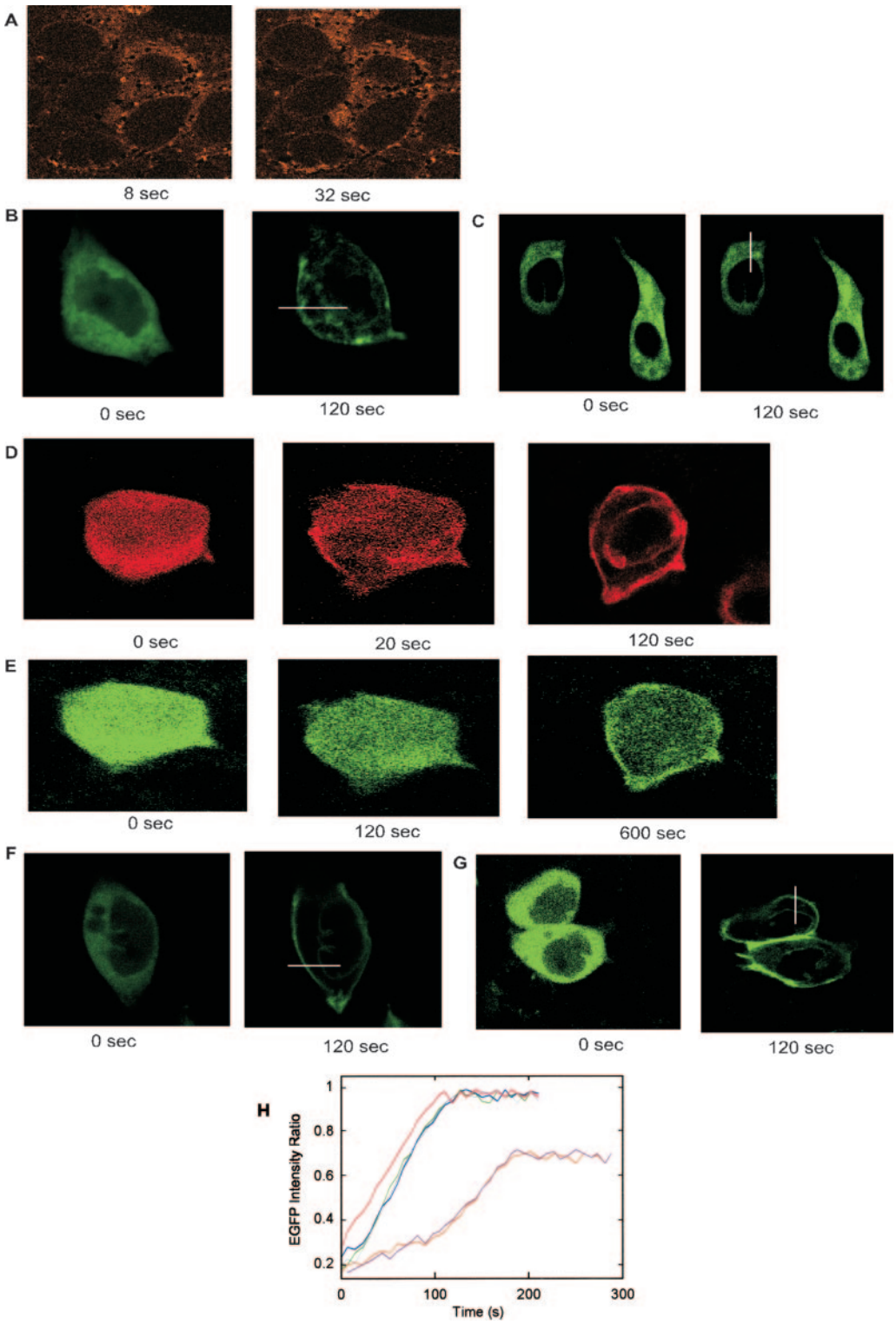

FIG. 7. **Membrane translocation and cellular distribution of EGFP-tagged PKCδ, PKCε and mutants in response to OPG treatment.** *A–G*, HEK293 cells were treated with 0.1 mg/ml OPG and two-photon images of OPG (*A*), PKCε-EGFP (*B*), PKCδ-EGFP (*C*), PKCε-HcRed (*D*), PKCδ-EGFP (*E*), PKCε D188A-EGFP (*F*), and PKCε D257A-EGFP (*G*) were taken every 7 s. Lines shown here represent one of three lines drawn in each cell for calculating subcellular distribution of EGFP intensity (see Fig. 8). In *D* and *E*, PKCε-HcRed and PKCδ-EGFP were cotransfected into HEK293 cells and simultaneously monitored. *H*, the time-lapse changes in EGFP intensity ratio at the plasma membrane (= plasma membrane/[plasma membrane + cytoplasm]) are shown for PKCε wild type (*cyan*), D188A (*green*), W191G (*orange*), D257A (*blue*), W264G (*purple*), and ΔC2 (*red*).

showed that fluorogenic OPG is spontaneously distributed to the intracellular membranes, because its lipophilicity is lower than that of natural DAGs with longer acyl chains (23). Fig. 7 shows the time-lapse images of OPG and EGFP-tagged proteins in representative cells, each selected from >10 cells showing a similar pattern. A minimum of quadruple measurements were performed for each protein with >5 cells monitored for each measurement. Typically, >80% of cell population showed similar behaviors with respect to DAG-induced PKCε translocation. As reported previously, OPG was rapidly distributed to

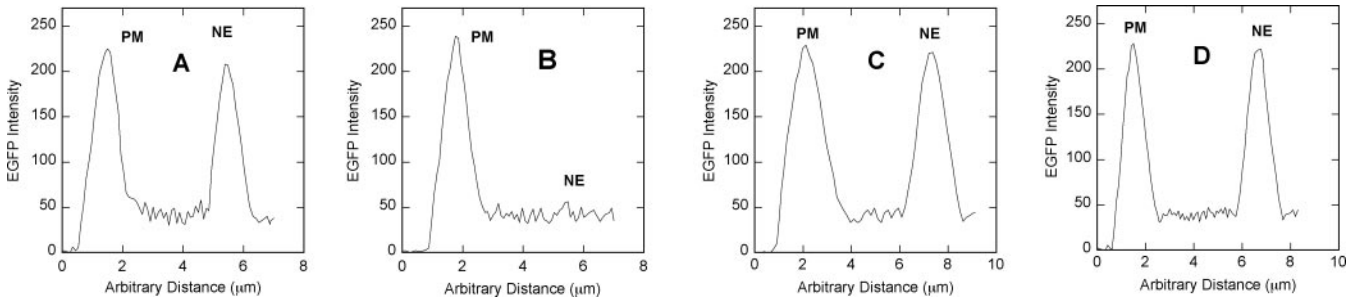

FIG. 8. **Subcellular distribution of EGFP intensity after OPG addition to HEK293 cells.** EGFP intensity profiles were determined from Fig. 7 as described under "Experimental Procedures." The differential subcellular localization patterns are shown for PKCε wild type (n = 15) (*A*), PKCδ wild type (n = 15) (*B*), PKCε D188A (n = 10) (*C*), and PKCε D257A (n = 10) (*D*) 7 min after OPG addition. *PM* and *NE* indicate plasma membrane and nuclear envelope, respectively.

TABLE III

Affinity of PKCε and mutants for cell membrane mimics determined from SPR analysis

Values represent the mean and standard deviation from three determinations. All measurements were performed in 10 mM HEPES, pH 7.4, containing 0.16 M KCl.

Proteins	k_a	k_d	K_d[a]	PM specificity[b]
	$M^{-1}\ s^{-1}$	s^{-1}	M	
Inner Plasma membrane mimetic: POPC/POPE/POPS/POPI/cholesterol/DiC_{18} (12:35:22:9:21:1)				
PKCε	$(1.2 \pm 0.3) \times 10^7$	$(1.5 \pm 0.4) \times 10^{-2}$	$(1.2 \pm 0.4) \times 10^{-9}$	1.8
D188A	$(1.2 \pm 0.2) \times 10^7$	$(1.3 \pm 0.4) \times 10^{-2}$	$(1.1 \pm 0.4) \times 10^{-9}$	1.6
D257A	$(1.4 \pm 0.4) \times 10^7$	$(2.7 \pm 0.6) \times 10^{-2}$	$(1.9 \pm 0.7) \times 10^{-9}$	1.3
Nuclear membrane mimetic: POPC/POPE/POPS/POPI/cholesterol/DiC_{18} (61:21:4:7:6:1)				
PKCε	$(8.9 \pm 0.9) \times 10^5$	$(1.9 \pm 0.3) \times 10^{-3}$	$(2.1 \pm 0.4) \times 10^{-9}$	
D188A	$(9.6 \pm 1.1) \times 10^5$	$(1.7 \pm 0.2) \times 10^{-3}$	$(1.8 \pm 0.3) \times 10^{-9}$	
D257A	$(8.6 \pm 0.7) \times 10^5$	$(2.1 \pm 0.4) \times 10^{-3}$	$(2.4 \pm 0.5) \times 10^{-9}$	

[a] K_d determined by k_d/k_a for these measurements.
[b] Ratio of $(1/K_d)$ for the plasma membrane mimetic to $(1/K_d)$ for the nuclear envelope mimetic.

all cellular membranes within 10 s when added to the cells (Fig. 7*A*). In response to OPG stimulation, wild type PKCε-EGFP instantaneously translocated to both the plasma membrane and the perinuclear region (Fig. 7*B*). This translocation is much faster than the plasma membrane translocation of PKCδ-EGFP under the same conditions (Fig. 7*C*), which is consistent with the notion that C1 domains of PKCε are conformationally unrestricted and their DAG binding sites are readily accessible. To further demonstrate that PKCε translocation is much more rapid than that of PKCδ under the same conditions, we simultaneously monitored the membrane translocation of PKCε-HcRed and PKCδ-EGFP in the same cells. As shown in Fig. 7 (*D* and *E*), HcRed-labeled PKCε translocated to membranes much faster than EGFP-labeled PKCδ in response to OPG addition. This difference was not due to different fluorescence proteins, because PKCε-HcRed and PKCε-EGFP showed essentially the same *in vitro* vesicle affinities (data not shown).

Quantitative evaluation of EGFP intensity throughout the cell confirmed the comparable PKCε localization at the plasma membrane and the perinuclear region (see Fig. 8*A*). Similar results were obtained when HEK293 cells were activated by DiC_8 in lieu of OPG (data not shown). This multisite membrane targeting of PKCε is again in stark contrast with PKCδ that translocates exclusively to the plasma membrane under the same conditions (Fig. 8*B*). The specific translocation of PKCδ to the plasma membrane with omnipresent OPG (or DiC_8) was attributed to its strong preference for lipid headgroup composition of the inner plasma membrane over other intracellular membranes (23). To see if the nonspecific subcellular localization of PKCε is due to lack of preference for any particular cellular membrane, we measured its binding to vesicle mimetics of the inner plasma membrane and nuclear envelope containing 1 mol% DiC_{18} by the SPR analysis. As listed in Table III, PKCε binds the plasma membrane (K_d = 1.2 nM) and nuclear membrane mimetics (K_d = 2.1 nM) with comparable affinity. Under the same conditions, PKCδ showed 50-fold preference for the plasma membrane mimetic over the nuclear membrane mimetic (23). Thus, it appears that divergent subcellular localization of PKCδ and PKCε is due at least in part to their distinctively different lipid headgroup selectivity.

We also measured OPG (or DiC_8)-mediated subcellular localization of PKCε mutants. All PKCε mutants exhibited the same dual subcellular localization pattern as the wild type PKCε (see Figs. 7*F*, 7*G*, 8*C*, and 8*D*). We then determined the rates of OPG-induced plasma membrane translocation for wild type and mutants from the analysis of EGFP intensity *versus* time plots (see Fig. 7*G*). Similar studies on other membrane targeting domains and membrane binding proteins showed good correlation between their *in vitro* vesicle affinity and cellular membrane translocation rates (31). In accordance with their wild type-like *in vitro* membrane binding properties (see Tables I and III), D188A (see also Fig. 7*F*) and D257A (see also Fig. 7*G*) translocated to the plasma membrane (and to the perinuclear region) as fast as the wild type. In the case of PKCδ, corresponding mutations were shown to dramatically enhance the translocation rate (23). We also found that the C1A and C1B hydrophobic site mutants (W191G and V193G in the C1A and W264G and L266G in the C1B) migrated to the membrane much slower than wild type (Fig. 7*H*), which is again consistent with our *in vitro* membrane binding data. Thus, it would seem that both the C1A and C1B domains play an important role in both *in vitro* and cellular DAG-mediated membrane binding of PKCε. The ΔC2 construct showed slightly faster membrane translocation than wild type (Fig. 7*H*), corroborating the notion

that the C2 domain does not play a major role in membrane targeting of PKCε.

DISCUSSION

Extensive studies have been performed to understand the mechanisms by which PKC isoforms are differentially targeted and regulated in the cells, as elucidation of such mechanisms will lead to new strategies for controlling of specific PKC isoforms and cellular processes mediated by these enzymes. The present study reveals how differently two novel PKC isoforms, PKCδ and PKCε, are targeted and activated in the cell. The novel PKC family can be further subdivided into two groups, δ/θ group and ε/η group, based on sequence similarity. Although functional similarities within and differences between the two novel PKC groups have not been firmly established, PKCδ and PKCε have been reported to have opposing functions and different regulatory mechanisms in mammalian cells (10–12).

Our isothermal titration calorimetry measurements of isolated C1 domains clearly show that both C1 domains of PKCε can bind DAG with high affinity, whereas only the C1A domain of PKCδ has high DAG affinity. Furthermore, our SPR and monolayer analyses of PKCε and mutants (D188A and D245A) indicate that the C1 domains of PKCε are conformationally unrestricted and readily accessible to DAG, unlike the C1 domains of PKCδ that are intramolecularly tethered via Glu^{177} and Asp^{245}, respectively. Our recent study on PKCα and PKCγ delineated the relationship between PS selectivity of PKC and the conformational flexibility of its C1 domains: *i.e.* PS selectivity derives from its capability to specifically relieve the intramolecular tethering of C1 domains (22). In accordance with this notion, PKCε showed little PS selectivity, whereas PKCδ had pronounced selectivity for PS over PG.

Due to comparably high DAG affinities and conformational flexibility, both C1A and C1B domains of PKCε are involved in the membrane binding of this isoform, as evidenced by the similar reducing effects of mutations of the C1A and C1B hydrophobic residues on the vesicle binding and monolayer penetration of PKCε. The effect of the double mutation of the C1A and C1B domains on the vesicle and monolayer binding of PKCε indicates that its two C1 domains work additively rather than synergistically. Furthermore, our activity measurements of these hydrophobic site mutants suggest that, although the C1A and C1B domains make comparable contributions to membrane binding of PKCε, the partial membrane penetration of the C1A domain is more important for removal of the pseudosubstrate region from the active site of PKCε than that of the C1B domain because of the proximity between the C1A domain and the pseudosubstrate sequence (see Fig. 1).

Then, what causes the major functional differences between the C1 domains of PKCδ and PKCε? The lack of the high resolution structure of C1·DAG complex does not allow us to pinpoint the structural determinant that causes different DAG affinities of C1 domains; however, the DAG affinity differences are expected to derive from the structural variation in the ligand-binding pocket. It is even more difficult to account for the different conformational flexibility of C1 domains. The C1A and C1B domains of PKCε contain Asp residues whose counterparts in PKCδ play a key role in intramolecular tethering of its C1A and C1B domains (23). Because the deletion of C2 domain has no significant effect on both PKCδ and PKCε, it does not seem that the different dynamic properties of PKCδ and PKCε C1 domains derive from different degrees of intramolecular interactions with their C2 domains. Our preliminary modeling suggests that C1A and C1B domains of PKCδ, but not those of PKCε, may form an interdomain interaction owing to their electrostatic and hydrophobic complementarity.[2] Obviously, further studies are needed to determine the nature of intramolecular interactions that limit the DAG accessibility of PKCδ C1 domains, which is beyond the scope of this investigation.

One of common properties shared by PKCδ and PKCε is low membrane binding affinity of their C2 domains. Significant structural differences between the C2 domains of PKCδ and PKCε suggest that they might have different functional properties. In particular, it has been proposed that the C2 domain of PKCε contributes to the overall membrane affinity of PKCε, either through specific interaction with phosphatidic acid (42) or through phosphorylation-enhanced interaction with phospholipids (43). Although the isolated C2 domain of PKCε has higher affinity for anionic vesicles than that of PKCδ, its overall vesicle affinity is <1% of the full-length PKCε and is not enhanced by a phosphorylation-mimicking mutation. Also, it shows only modest selectivity for POPC/POPA (7:3) over POPC/POPS (7:3) vesicles, which may be simply due to the stronger anionic property of phosphatidic acid-containing vesicles. Thus, it would seem that the C2 domains of PKCδ and PKCε do not directly contribute to the membrane binding of their host proteins.

The structural and functional differences between PKCδ and PKCε have great impact on their subcellular targeting and activation. Due to the ready accessibility of its C1 domains, PKCε translocates to the membrane much faster than PKCδ in response to exogenous DAG addition in HEK293 cells. Also, PS-independent PKCε randomly translocates to cellular membranes when DAG is fed into all cell membranes of HEK293 cells, whereas PS-selective PKCδ is specifically targeted to the PS-rich inner plasma membrane under the same conditions. Thus, under the physiological conditions PKCε should respond much faster than PKCδ to the receptor-generated DAG formation in the plasma membrane and may also be able to bind DAG in other intracellular membranes, such as Golgi apparatus and endoplasmic reticulum. This difference may play a significant role in their divergent cellular targeting and activation.

It has been reported that PKC adaptor proteins (*e.g.* RACK) are associated with the subcellular localization of PKC isoforms (45). For PKCε, it has been proposed that εRACK located in the Golgi complex mediates the targeting of PKCε by interacting with its C2 domain (18). Although direct binding of PKCε with εRACK (or any peptides derived from εRACK) has not been quantitatively demonstrated, cell studies using peptides provided evidence that the C2 domain of PKCε contains a RACK binding site that is intramolecularly shielded by another part of the C2 domain, termed the ψ-RACK site (46). A recent report showed that a PKCε mutant with putatively disrupted intramolecular interaction translocated to the plasma membrane significantly faster than the wild type in CHO cells upon PMA addition or ATP stimulation (47). As described above, the deletion of the C2 domain has no significant effect on the *in vitro* and cellular membrane binding properties of PKCε under our experimental conditions, indicating that the C2 domain does not play a major role in the membrane binding of PKCε. It is difficult to evaluate the contribution of putative C2-εRACK binding to the translocation efficiency of PKCε using a cell system overexpressing PKCε due to the non-stoichiometric presence of PKCε and εRACK. Therefore, the present study is not necessarily at odds with the notion that εRACK plays an important role in subcellular localization of PKCε. Given its promiscuous lipid headgroup specificity and tendency to non-selectively translocate to any DAG-containing intracellular

[2] R. Stahein, D. Murray, and W. Cho, unpublished observation.

membranes, the presence of εRACK can be particularly advantageous and even necessary for PKCε.

Acknowledgment—We thank Dr. Diana Murray for preliminary modeling work on PKCδ and PKCε C1A and C1B domains.

REFERENCES

1. Parekh, D. B., Ziegler, W., and Parker, P. J. (2000) *EMBO J.* **19,** 496–503
2. Newton, A. C. (2001) *Chem. Rev.* **101,** 2353–2364
3. Shirai, Y., and Saito, N. (2002) *J. Biochem.* (*Tokyo*) **132,** 663–668
4. Brose, N., and Rosenmund, C. (2002) *J. Cell Sci.* **115,** 4399–4411
5. Yang, C., and Kazanietz, M. G. (2003) *Trends Pharmacol. Sci.* **24,** 602–608
6. Cho, W. (2001) *J. Biol. Chem.* **276,** 32407–32410
7. Nalefski, E. A., and Falke, J. J. (1996) *Protein Sci.* **5,** 2375–2390
8. Rizo, J., and Sudhof, T. C. (1998) *J. Biol. Chem.* **273,** 15879–15882
9. Akita, Y. (2002) *J. Biochem.* (*Tokyo*) **132,** 847–852
10. Mischak, H., Goodnight, J. A., Kolch, W., Martiny-Baron, G., Schaechtle, C., Kazanietz, M. G., Blumberg, P. M., Pierce, J. H., and Mushinski, J. F. (1993) *J. Biol. Chem.* **268,** 6090–6096
11. Chen, L., Hahn, H., Wu, G., Chen, C. H., Liron, T., Schechtman, D., Cavallaro, G., Banci, L., Guo, Y., Bolli, R., Dorn, G. W., 2nd, and Mochly-Rosen, D. (2001) *Proc. Natl. Acad. Sci. U. S. A.* **98,** 11114–11119
12. Liu, H., McPherson, B. C., and Yao, Z. (2001) *Am. J. Physiol.* **281,** H404–H410
13. Rodriguez, M. M., Chen, C. H., Smith, B. L., and Mochly-Rosen, D. (1999) *FEBS Lett.* **454,** 240–246
14. Numazaki, M., Tominaga, T., Toyooka, H., and Tominaga, M. (2002) *J. Biol. Chem.* **277,** 13375–13378
15. Uberall, F., Giselbrecht, S., Hellbert, K., Fresser, F., Bauer, B., Gschwendt, M., Grunicke, H. H., and Baier, G. (1997) *J. Biol. Chem.* **272,** 4072–4078
16. Newton, A. C. (2003) *Biochem. J.* **370,** 361–371
17. Kashiwagi, K., Shirai, Y., Kuriyama, M., Sakai, N., and Saito, N. (2002) *J. Biol. Chem.* **277,** 18037–18045
18. Csukai, M., Chen, C. H., De Matteis, M. A., and Mochly-Rosen, D. (1997) *J. Biol. Chem.* **272,** 29200–29206
19. Prekeris, R., Mayhew, M. W., Cooper, J. B., and Terrian, D. M. (1996) *J. Cell Biol.* **132,** 77–90
20. Medkova, M., and Cho, W. (1999) *J. Biol. Chem.* **274,** 19852–19861
21. Bittova, L., Stahelin, R. V., and Cho, W. (2001) *J. Biol. Chem.* **276,** 4218–4226
22. Ananthanarayanan, B., Stahelin, R. V., Digman, M. A., and Cho, W. (2003) *J. Biol. Chem.* **278,** 46886–46894
23. Stahelin, R. V., Digman, M. A., Medkova, M., Ananthanarayanan, B., Rafter, J. D., Melowic, H. R., and Cho, W. (2004) *J. Biol. Chem.* **279,** 29501–29512
24. Kates, M. (1986) *Techniques of Lipidology*, 2nd Ed., pp. 114–115, Elsevier, Amsterdam
25. Sunamoto, J., Kondo, H., Nomura, T., and Okamoto, H. (1980) *J. Am. Chem. Soc.* **102,** 1146–1152
26. Ho, S. N., Hunt, H. D., Horton, R. M., Pullen, J. K., and Pease, L. R. (1989) *Gene* (*Amst.*) **77,** 51–59
27. Medkova, M., and Cho, W. (1998) *Biochemistry* **37,** 4892–4900
28. Cho, W., Digman, M., Ananthanarayanan, B., and Stahelin, R. V. (2003) *Methods Mol. Biol.* **233,** 291–298
29. Cho, W., Bittova, L., and Stahelin, R. V. (2001) *Anal. Biochem.* **296,** 153–161
30. Stahelin, R. V., and Cho, W. (2001) *Biochemistry* **40,** 4672–4678
31. Stahelin, R. V., Rafter, J. D., Das, S., and Cho, W. (2003) *J. Biol. Chem.* **278,** 12452–12460
32. Newton, A. C. (1993) *Annu. Rev. Biophys. Biomol. Struct.* **22,** 1–25
33. Newton, A. C., and Keranen, L. M. (1994) *Biochemistry* **33,** 6651–6658
34. Mozsolits, H., Thomas, W. G., and Aguilar, M. I. (2003) *J. Pept. Sci.* **9,** 77–89
35. Bazzi, M. D., and Nelsestuen, G. L. (1988) *Biochemistry* **27,** 6776–6783
36. Irie, K., Oie, K., Nakahara, A., Yanai, Y., Ohigashi, H., Wender, P. A., Fukuda, H., KOnishi, H., and Kikkawa, U. (1998) *J. Am. Chem. Soc.* **120,** 9159–9167
37. Slater, S. J., Ho, C., Kelly, M. B., Larkin, J. D., Taddeo, F. J., Yeager, M. D., and Stubbs, C. D. (1996) *J. Biol. Chem.* **271,** 4627–4631
38. Bogi, K., Lorenzo, P. S., Szallasi, Z., Acs, P., Wagner, G. S., and Blumberg, P. M. (1998) *Cancer Res.* **58,** 1423–1428
39. Newton, A. C. (1995) *Curr. Biol.* **5,** 973–976
40. Medkova, M., and Cho, W. (1998) *J. Biol. Chem.* **273,** 17544–17552
41. Pappa, H., Murray-Rust, J., Dekker, L. V., Parker, P. J., and McDonald, N. Q. (1998) *Structure* **6,** 885–894
42. Ochoa, W. F., Garcia-Garcia, J., Fita, I., Corbalan-Garcia, S., Verdaguer, N., and Gomez-Fernandez, J. C. (2001) *J. Mol. Biol.* **311,** 837–849
43. Pepio, A. M., and Sossin, W. S. (2001) *J. Biol. Chem.* **276,** 3846–3855
44. Jose Lopez-Andreo, M., Gomez-Fernandez, J. C., and Corbalan-Garcia, S. (2003) *Mol. Biol. Cell* **14,** 4885–4895
45. Csukai, M., and Mochly-Rosen, D. (1999) *Pharmacol. Res.* **39,** 253–259
46. Dorn, G. W., 2nd, Souroujon, M. C., Liron, T., Chen, C. H., Gray, M. O., Zhou, H. Z., Csukai, M., Wu, G., Lorenz, J. N., and Mochly-Rosen, D. (1999) *Proc. Natl. Acad. Sci. U. S. A.* **96,** 12798–12803
47. Schechtman, D., Craske, M. L., Kheifets, V., Meyer, T., Schechtman, J., and Mochly-Rosen, D. (2004) *J. Biol. Chem.* **279,** 15831–15840

Diacylglycerol-induced Membrane Targeting and Activation of Protein Kinase C?: MECHANISTIC DIFFERENCES BETWEEN PROTEIN KINASES C δ AND C?

Robert V. Stahelin, Michelle A. Digman, Martina Medkova, Bharath Ananthanarayanan, Heather R. Melowic, John D. Rafter and Wonhwa Cho

J. Biol. Chem. 2005, 280:19784-19793.
doi: 10.1074/jbc.M411285200 originally published online March 15, 2005
